Improvement of inverted planar heterojunction solar cells efficiency by using KI/Alq3 hybrid exciton blocking layer

Hind Lamkaouane, Hajar Ftouhi, Mimoun Zazoui, Mohammed Addou, Linda Cattin, Jean-Christian Bernède, Guy Louarn, Yamina Mir

Version of Record: https://www.sciencedirect.com/science/article/pii/S0038110121002082
Manuscript_6046030c16b72ac3e9dbbae85066059c

Improvement of inverted planar heterojunction solar cells efficiency by using KI/Alq_3 hybrid exciton blocking layer.

Hind Lamkaouane[1,2*], Hajar Ftouhi[1,4], Mimoun Zazoui[2], Mohammed Addou[4], Linda Cattin[1], Jean Christian bernède[3], Guy Louarn[1], Yamina Mir[2].

[1]Université de Nantes, Institut des Matériaux Jean Rouxel (IMN), CNRS, UMR 6502, Université de Nantes, 2 rue de la Houssinière, BP 32229, 44322 Nantes cedex 3, France

[2]Laboratoire de physique de la matière condensée et énergies renouvelables, faculté des sciences et techniques. Mohammedia. Université Hassan II de Casablanca B.P 146, Mohammedia, Morocco.

[3]MOLTECH-Anjou, CNRS, UMR 6200, Université de Nantes, 2 rue de la Houssinière, Nantes F-44322 France

[4]Équipe de Recherche Couches Minces et Nanomatériaux – Faculté des Sciences et Techniques, Université Abdelmalek Essaâdi, BP : 416. Tanger - Maroc

Abstract

The exciton blocking layer (EBL) as an interfacial layer is extremely critical in determining the organic photovoltaic cell (OPV) performances. Here, we studied inverted planar heterojunction solar cells PHJ-OPVs with the following configuration ITO/EBL/C_{60}/CuPc/MoO_3/Al. Upon the EBL functionality which can act as an exciton blocking layer and allows the electron collection at the cathode, we proposed the insertion of hybrid EBL consisted of KI/Alq_3 thin layer**.** The Alq_3 is known as an EBL due to its broad bandgap, whereas we found that when a thin layer of 1nm of KI is introduced in ITO/Alq_3 interface, the KI decomposed during the thermal deposition, and only potassium interacts and diffuses in the Alq_3 layer, which effectively enhances the electrons collection at the ITO/C_{60} interfaces leading to the improvement of open-circuit voltage (Voc), and device power conversion efficiency by 36% than the device using Alq_3 alone as EBL.

Keywords

Inverted organic solar cell, planar heterojunction, hybrid thin film, exciton blocking layer, KI thin layer, vacuum thermal deposition.

1. Introduction

Organic photovoltaic cells (OPVs) are among the most studied and interesting technology in the photovoltaic field due to their many advantages such as low cost, lightweight, large area, and flexibility [1][2]. Recently, wide attention has been paid to bulk heterojunction solar cells (BHJs) for increasing their efficiency[3][4]. BHJs are considered as one of the effective cells owing to development of new organic materials replacing the fullerene derivative[5][6]. As a matter of fact, it is known that "champion OPVs"-are issued from the family of the BHJ-OPVs due to the larger area of the interface between the electron donor and the electron acceptor [7]. In recent times, dramatic advances of the performances of OPVs have been achieved using new promising molecules and polymers, mainly non fullerene acceptors (NFA) [8][9][10]. Nevertheless, it is difficult to obtain reproducible results with BHJs because it is complicated to control the morphology of the blend, while, with time, there is progressive phase separation and performance degradation[11]. Moreover, the synthesis of the new materials such as NFAs is not trivial. Thus, in the near future, it would be difficult to transfer the lab-scale device fabrication to that of the industry. It is therefore interesting to study the performances of cells using small molecules, although less efficient, but easier to obtain with perfectly controlled synthesis and reproducible properties [12][13][14][15].So, the spirit of our study is to seek to understand how OPVs work so as to propose new possibilities for improving their performance in the future. Planar heterojunctions are well suited for investigating new materials, as materials can be characterized independently before device fabrication and many parameters, such as light absorption and film morphology, can be determined experimentally. In the present work, in a first time we used a very classical well known and cheap dye, CuPc, even if its limits are known, to test the validity, or not, of our new hybrid exciton blocking layer (EBL). Then, it will be possible to use some more performing molecule, where upon some more sophisticated process, such as co-evaporation to form BHJ in order to try improving the efficiency of the structures. For instance, the results obtained by "Heliatek" prove that significant improvement can be obtained through use of "pin" structures deposited under vacuum [16].

PHJ-OPVs contain two organic semiconductors, an electron donor (ED) and an electron acceptor (EA). Both stacked layers are inserted between two electrodes, the cathode top electrode is characterized by low work function and high reflectivity as Aluminum (Al), the second is the bottom anode electrode with high work function and high transparency as indium thin oxide (ITO). One of the important factors to achieve a high efficiency is a good band matching between the organic semiconductors and electrodes, which implies that the energy offset should be minimized between the

donor's HOMO, the acceptor's LUMO and the work function of anode and the cathode respectively [17]. On the other hand, classical PHJ-OPVs lifetime is affected mainly by environmental conditions. Actually, the moisture and oxygen could diffuse through the cathode and cause irreversible electronic structure modifications of the acceptor underlayer. Fullerene (C_{60}) is the most used as acceptor material and it is highly sensitive to ambient atmosphere leading to quite fast OPV degradation [18][19][20]. Encapsulation and introduction of interfacial layer between the low work function metal and the photoactive layer are possible ways to protect the fullerene (C_{60}) [21][22]. Another approach to improve the OPVs lifetime and stability is to use an inverted configuration, where the acceptor material is deposited under the donor material preventing its oxidation and therefore the cells degradation [18]. Moreover, the insertion of thin buffer layer is not only beneficial in terms of power conversion efficiency enhancement but also in terms of device stability [21][22].

In this study, we focused on the enhancement of the interfacial layer between the organic acceptor layer and the cathode using cathode buffer layer named exciton blocking layer (EBL). This thin layer has the ability to block the excitons, preventing any exciton quenching by the cathode [23]. Bathocuproine (BCP) and Tris-(8-hydroxyquinoline) (Alq_3) have already been used as efficient EBLs [23][24][25][26][27]. However, the BCP is not stable as much as Alq_3 towards the moist environment. Thus, the Alq_3 is beneficial for efficiency improvement and lifetime [21][28][29].

In the present work, inverted PHJ-OPVs based on fullerene and copper phthalocyanine (C_{60}/CuPc) as photoactive layers were investigated. MoO_3 thin layer is well known as an anode buffer layer. So it has been selected as an interfacial layer to improve the hole extraction at the anode/ electron donor interface [30][31][18].ITO/EBL/C_{60}/CuPc/MoO_3/Al is the structure of the inverted PHJ-OPV studied here (Fig.1). In classical configuration, the EBL is chosen to block the excitons at the cathode/ electron acceptor interface. Moreover, it prevents metal diffusion into the electron acceptor layer during cathode deposition. Also, it allows better extraction of electrons from the acceptor material towards the cathode [23]. Alq_3 with a wide band gap (3 eV) is considered as a good EBL with an optimal thickness of 9 nm. Such thickness is too high to permit the passage of the electrons by tunnel effect [22]. Instead of the tunnel effect mechanism, the electron transport mechanism in classical configuration is explained by another physical process, where the electrons transport takes place by means of channels induced by metal-diffusion during the cathode deposition [23][22]. At this point, the electron transport mechanism remains the challenge in inverted-PHJ, where no metal diffusion occurs in the EBL. To surpass this difficulty, some studies have been done to enhance the cathode/ acceptor interface using an ITO modified by mean of EBL such as ZnO and TiOx, which are often produced by wet chemical synthesis, the thins layers obtained could be an efficient EBL. However, these techniques have downsides as the difficulties in the thickness control and require additional temperature treatment to remove organic impurities [32][33][34][35]. Likewise, we can find EBLs produced by vacuum techniques such as ZnO: Al which showed good results compared with thin films

produced by processed solution [33]. Ag:BCP thin layer deposited by co-evaporation was also reported as an efficient EBL where the electron transport is ensured by a gap state generated by the interaction between the Ag, BCP, and C_{60}[18]. We have already shown that calcium is efficient with Alq_3 as double EBL [22]. CsI as cathode buffer layer contributes to a good ohmic contact at the cathode/C_{60} interface which permits to increase Voc [30].The good results obtained by our team on the use of potassium layer introduced in the EBL of the IOPV based on SubPc [36], motivated us to choose the potassium halide salts especially potassium iodide as the second layer with Alq_3 as EBL to achieve an efficient device with low cost. Moreover, KI is easier to manage than pure K, which has a higher sensitivity to oxidation. Potassium iodide is mostly used as an additive in perovskite solar cells, where the use of a small quantity could improve the perovskite crystallinity, reduce density in trap states and therefore enhance the device performance's[37].

Here in, a hybrid EBL based on KI and Alq_3 is proposed. This combination is supposed to improve the cell performance by enhancing the electron extraction from the C_{60} leading to the energy level alignments between the cathode work function and the LUMO of the acceptor thin layer by using potassium iodide (KI), while Alq_3 keeps the properties as a good exciton blocking layer. In this study, KI was incorporated at both interfaces ITO/Alq_3 and Alq_3/C_{60} with various thicknesses. We found that the OPVs performances were well enhanced when 1nm of KI thin layer was inserted in ITO/Alq_3 interface. The power conversion efficiency was improved by 36% and the open-circuit voltage by 25% in comparison with inverted PHJ-OPV without the inclusion of KI thin layer.

2. Experimental process

2.1 Organic photovoltaic cells deposition process

Inverted organic solar cells with the following structures ITO/EBL/C_{60}/CuPc/MoO_3/Al (Fig.1) were elaborated successfully by evaporation/sublimation under vacuum with a pressure of 10^{-6} mbar (all chemical products were supplied by CODEX). Before loading the substrates into the vacuum chamber, the 2/3 parts of the ITO coated glass substrate with a dimension of 25 mm x 25 mm and sheet resistance of 30 Ω were masked by using an adhesive tip. Then, the third part was chemically etched with Zn powder and hydrochloric acid (HCL) to obtain the under electrode. This step was followed by a cleaning with a dilute detergent solution and distilled water respectively. Then the ITO coated substrate was heated in an oven for 10 min after drying with a stream of air to clear out any trace of water. All layers were deposited successively without the need of breaking the vacuum. The thickness and the deposition rate of each layer were measured by a quartz monitor. First, the EBL was the double layer KI/Alq_3, Alq_3/KI, or then Alq_3 alone. The thickness of the KI thin layer was taken as parameter while the thickness of Alq_3 thin films was fixed at 9 nm. 0.01nm/s and 0.02 nm/s

were the growth rate of the KI thin layer and Alq_3, respectively. 0.04 nm/s and 0.09 nm/s were the growth rate, 30 nm and 40 nm were the thicknesses of CuPc and C_{60}, respectively. Then the MoO_3 thin layer was deposited with fixed thickness of 6 nm. At the last, Aluminum anode (Al) also was deposited *in situ* through shadow masks forming the cell active area which equals in our study 0.16 mm^2.

The inverted OPVs with the following structures were investigated, the device with Alq_3 alone as EBL was used here as reference cell.

$$\text{ITO (100 nm)} \Big/ \begin{matrix}\text{Alq3 (9nm)} \\ \text{KI (x nm)/Alq3 (9nm)} \\ \text{Alq3 (9nm)/KI (x nm)}\end{matrix} \Big/ \text{C60 (40 nm)} \Big/ \text{CuPc (30 nm)} \Big/ \text{MoO3 (6 nm)} \Big/ \text{Al (100 nm)}$$

The energy level diagram for the device with Alq3 thin layer alone, and with the hybrid KI/Alq3 as EBL are shown in Fig.2.

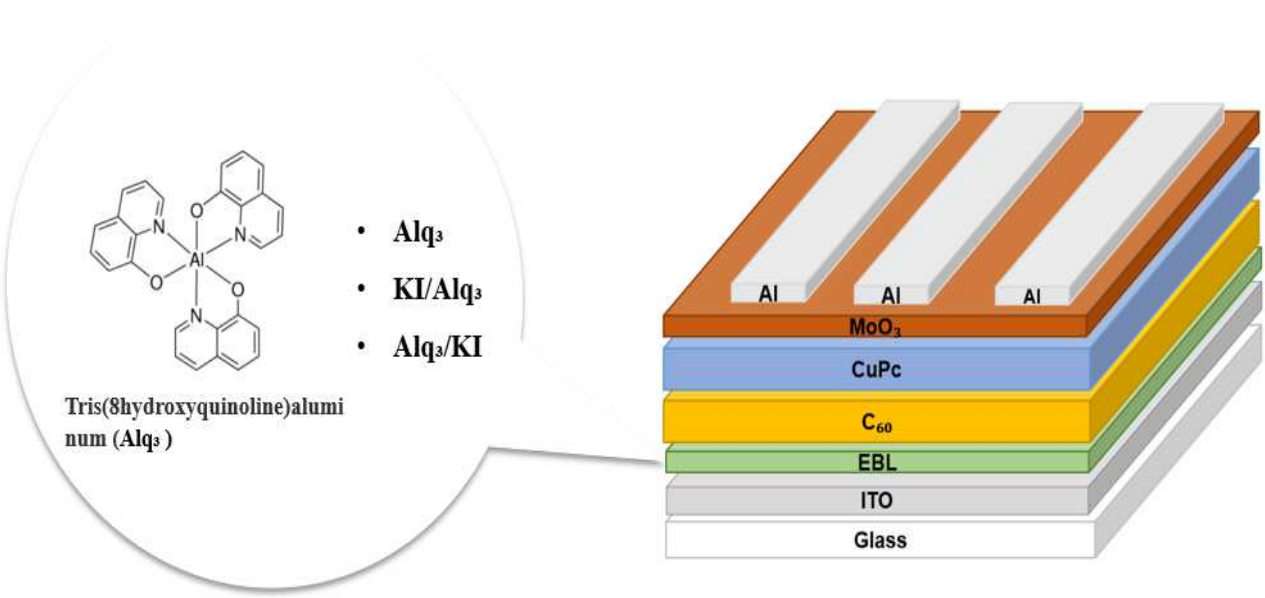

Fig.1.Schematic structure of inverted PHJ-OPV

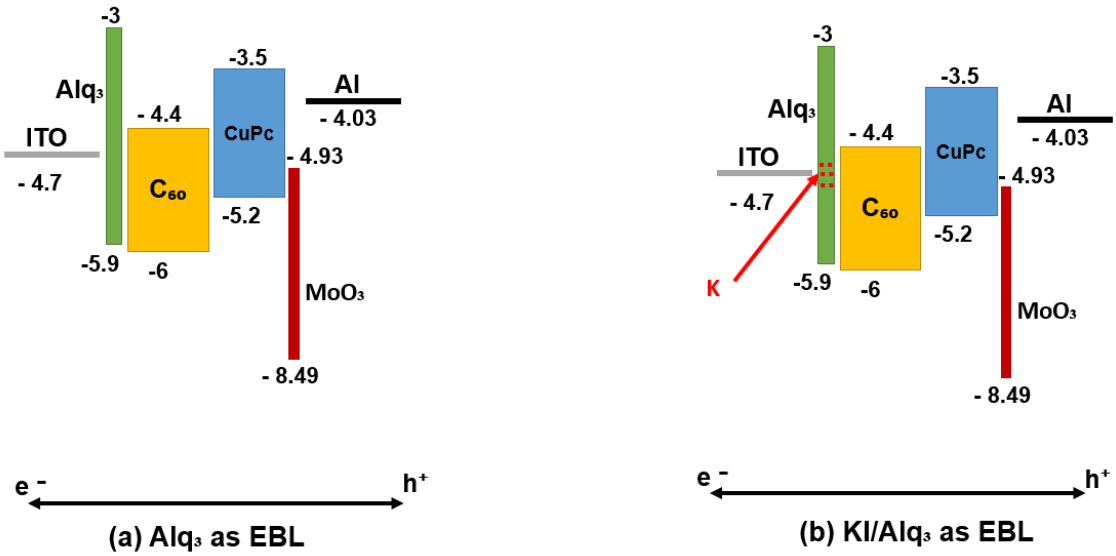

Fig.2.Energy level diagrams of Inverted PHJs (a) Alq3 as EBL and (b) KI/Alq3 as EBL

2.2 . Characterization techniques

The current density vs voltage (J-V) characteristics were measured at room temperature using J-V tester. The measurements were carried out with solar simulator (oriel 300 W) in the dark and under simulated AM 1.5 solar illumination. The external quantum efficiency measurements were carried out by an apparatus build up in our laboratory and the measurement of the incident photocurrent conversion efficiency were done with monochromatic continuous light without modulation. The surface morphology of the different films was visualized using a scanning electron microscope (SEM) JEOL 7600F with operating voltage 5kV, (Centre de microcaractéristion, Institut des Matériaux Jean Rouxel, Université de Nantes). The surface morphology of the thin films was measured by using atomic force microscopy (AFM) in tapping mode at room temperature, the instrument used for this study is dimension edge-barker, the cantilever has the following characteristics: Force constant of 10 to 130 N/m, Resonance frequency 204-497 KHz with a resistivity of 0.01-0.02 Ωcm. XPS measurements were taken by An Axis instrument from Kartos analytical spectrophotometer with Al Kα line (1486,6 eV) as excitation source has been used , the core level spectra were recorded with an energy step of 1eV, the C1s at binding energy 284.6 eV was considered as a reference.

Other techniques were used to characterize the thin films with and without KI thin layer, the structure was characterized by X-ray diffraction Siemens D8 diffractometer using CuKα radiation (Lambda Kα=0.15) and the UV-visible absorption spectra of the thins film were

measured at normal incidence in the spectral range 300nm - 800nm at room temperature using Perkin Elmer 3D WB Det.Module.

3. Results and discussion

The structures of PHJ devices are shown in Fig.1. After optimization of the reference OPV using Alq_3 alone, several cells were carried out to investigate the effect of potassium iodide thin layer on the cell performances as a function of its thickness in both ITO/Alq_3 and Alq_3/C_{60} interfaces. Fig.3 displays the current-voltage (J-V) curves of the elaborated cells with and without potassium iodide. The photovoltaic parameters, the power conversion efficiency (**η**), open-circuit voltage (Voc), current density (Jsc), series resistance (Rs), and shunt resistance (Rsh) are summarized in Table.1.

According to the results presented in Fig.3 and Table.1, it was found that the OPVs performances were improved significantly when a thin layer of KI is introduced at the ITO/Alq_3 interface. The best PCE of 2,2% was achieved by using KI/Alq_3 as EBL where the thickness of KI is only 1 nm. The Voc = 0,54 V and Jsc = 8,03 mA/cm^2, are significantly improved compared to the reference cell which has a Voc = 0,40 V, Jsc = 6,73 mA/cm^2. The efficiency of the reference OPV being 1,40%, and the efficiency of the OPV with KI/Alq_3 EBL, 2.2%, is improved by 36%.

When the thickness of the KI thin layer is 1.4 nm, good results were obtained. We can clearly observe a large increase in the fill factor to 58% due to the decrease of series resistance (2,2Ω), which is inversely proportional to the J(V) slope at the Voc point. The decrease of the series resistance can be assigned to lacks the traps in the electrodes/organic materials interfaces. However, the Voc is reduced, which induces a decrease in efficiency from 2.2 % to 1.97%.

In another hand, when the KI is inserted between the Alq_3 and the active layer, the results obtained by the two different cells using 1,6 nm or 0,2 nm have an efficiency of 1,41% and 1,48% respectively, which are quite homogenous compared with reference cell. It indicates that KI inserted between Alq_3/C_{60} interface does not significantly affect the power conversion efficiency.

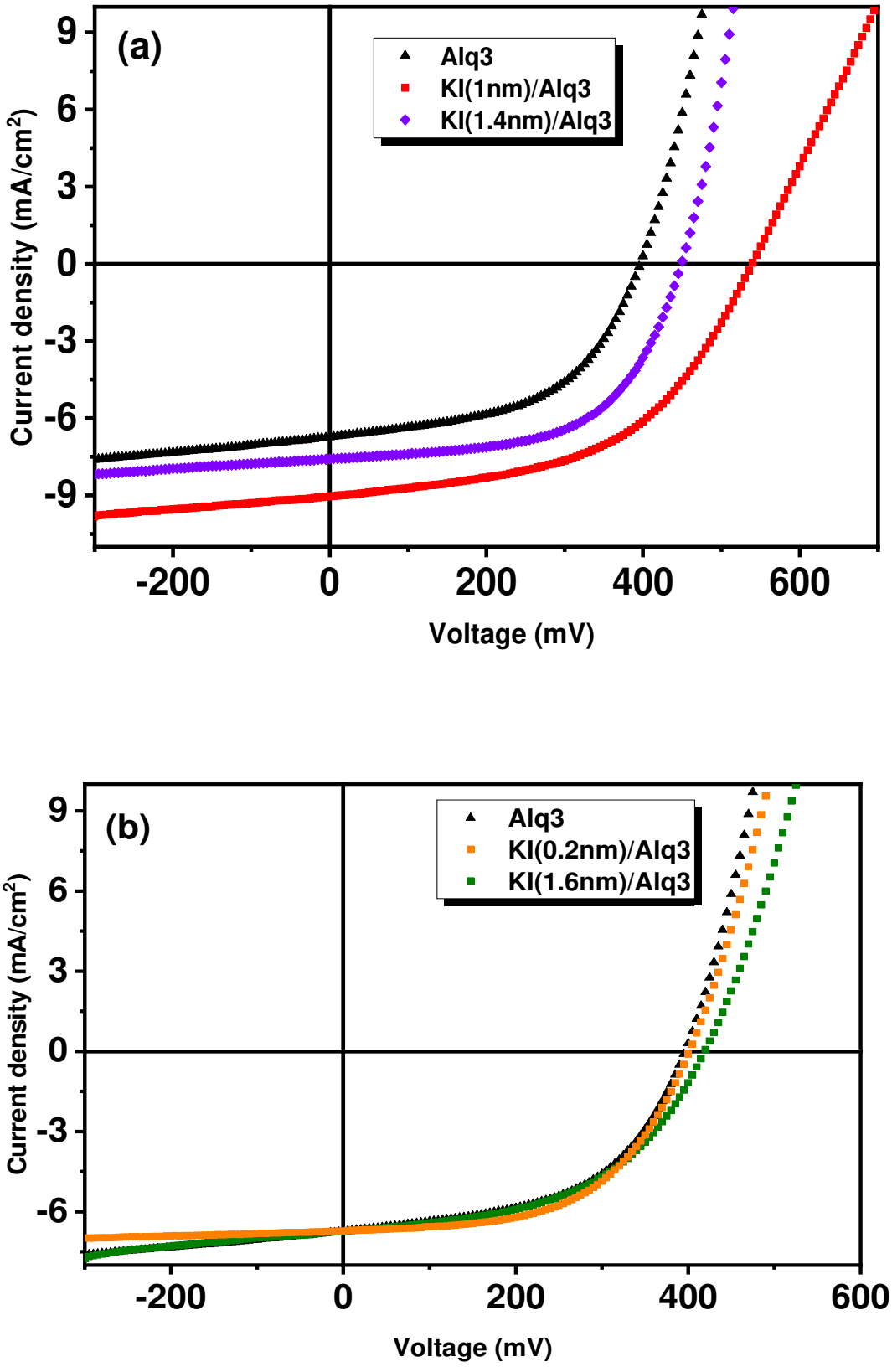

Fig.3. J-V characteristic of inverted PHJ with (a) KI/Alq$_3$and (b) Alq$_3$/KI as cathodes buffers layers.

Table 1. Photovoltaic parameters obtained from the J-V characteristic of the inverted PHJ-OPVs with different extracting buffer layers.

EBL	Thickness of KI (nm)	V_{oc}(V)	Jsc(mA/cm^2)	FF (%)	η (%)	Rs(Ω)	R_{sh}(Ω)
Alq_3	0	0.40	6.73	52.5	1.40	3	350
KI/Alq_3	1.4	0.45	7.58	58	1.97	2.2	520
	1	0.54	8.03	51	2.2	14	380
Alq_3/KI	1.6	0.419	6.13	50	1.41	4.5	340
	0.2	0.401	6.7	55	1.48	3.70	1000

The device using the hybrid KI/Alq_3 as EBL shows a higher short circuit current density value in comparison to the device without KI thin layer. To understand the origin of this improvement of the Jsc, we have measured the external quantum efficiency (EQE) for both cells. The EQE is extremely important for the device evaluation, which is complementary to the power conversion efficiency. It is defined as the ratio of the number of electrons collected by the photovoltaic cells to the number of incidents photons [38]. According to EQE spectra presented in Fig.4(a), both cells exhibit two photo-responses domains in the visible region: a photo-response located between 500nm and 800nm, and another one is located below 500 nm. As it is known, the EQE spectrum largely depends on the absorption of the photoactive layer. So, by comparison to the absorption spectra displayed in Fig. 4(b), we can attribute the first photo-response to the contribution of CuPc, while the second corresponds to the contribution of CuPc and C_{60}, showing that both layers contribute to the photocurrent generation. Moreover, the EQE signal of the inverted OPV with the hybrid EBL KI(1nm)/Alq_3 is increased on the whole wavelengths in the visible region by comparison with the OPV without KI thin layer. One can see that the total absorption of the active layer is slightly enhanced in the wavelength region from 550nm to 850nm when the KI thin layer was introduced (Fig.9(b)), which is in accordance with EQE enhancement. It can be concluded that the increase of the EQE justifies the Jsc improvement of the OPV with KI/Alq_3 as EBL.

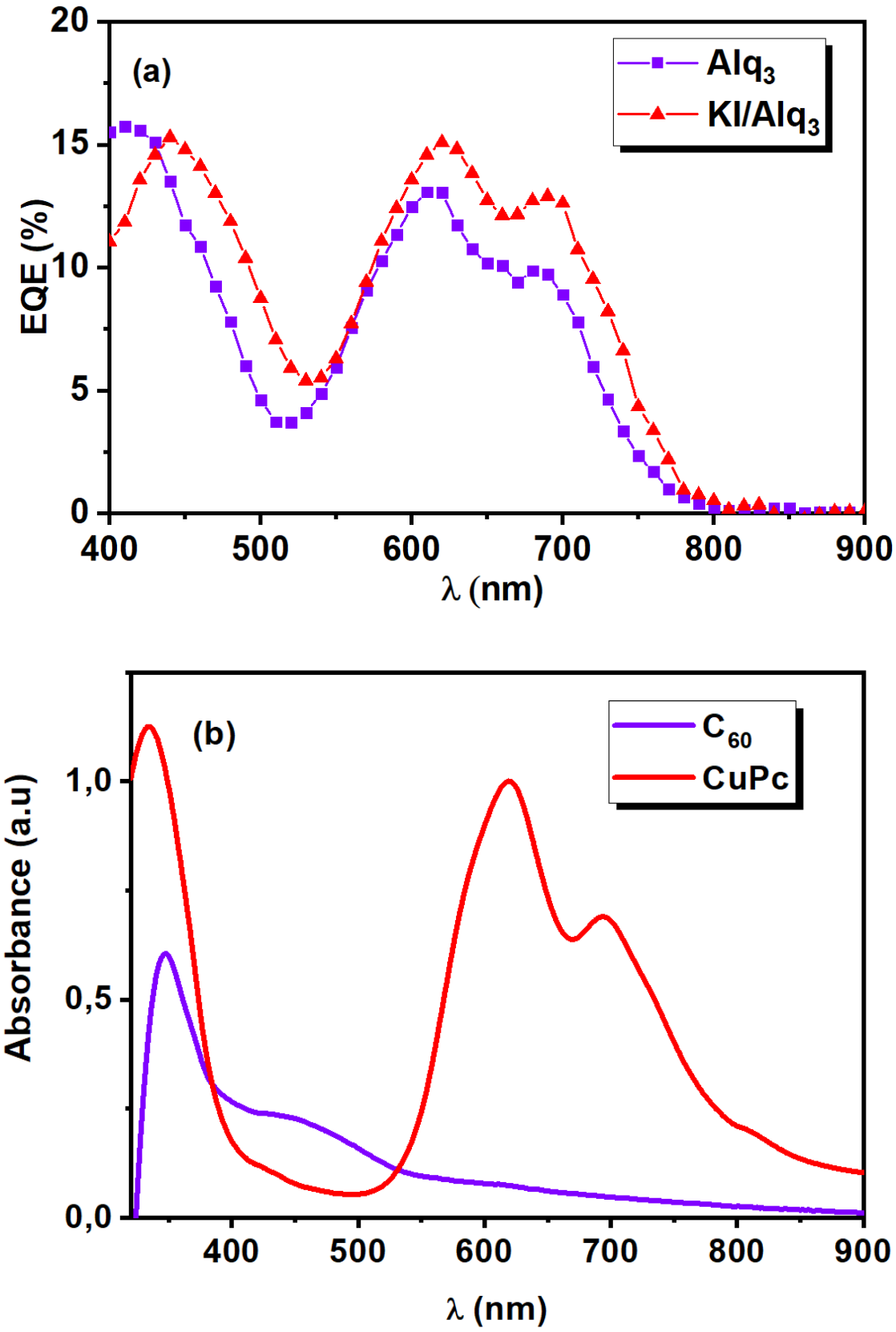

Fig.4. (a) EQE spectra of inverted PHJ-OPVs using KI/Alq_3 as EBL and the another using Alq3 alone and (b) absorption spectra of CuPc and C_{60} thin films.

To understand the improvement observed in the case of the cell using KI (1nm)/Alq_3 as EBL, we performed morphological characterization by scanning electron microscopy and atomic force microscopy, as well as chemical surface analysis by XPS which are important to rely between the optoelectronic properties and the photovoltaic performances [18]. The EBLs morphologies were investigated using AFM measurements. Fig. 5(a) and Fig. 5(b) represent the 2-dimensional AFM topographic images. From the 2D images, the Alq_3 surface deposited on ITO/KI is smooth and homogeneous as compared with the surface of Alq_3 deposited on bare ITO. The root mean square (rms) of the Alq_3 surface slightly decreased from 1.44 nm to 0.757 nm when 1 nm of KI is introduced, the rms and mean roughness are shown in Table.2. The surface smoothness can be considered as a good factor to minimize the interfacial charges recombination in the ITO/C_{60} interface [12].

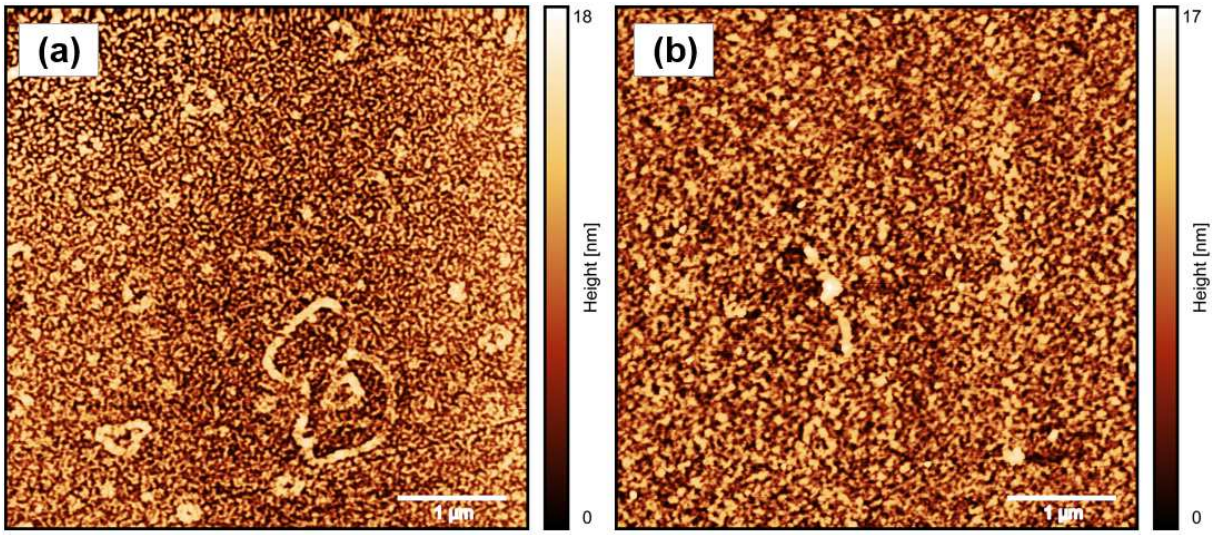

Fig.5. 2D AFM images(5µm x 5µm) of (a) ITO/Alq3 and (b) ITO/KI/Alq3.

Table 2. Rms and Ra of ITO/ETLs and ITO/ETLs/C60 where ETLs= Alq3 or KI/Alq_3.

EBLs	Area (5µmx5µm)		Area (10µmx 10µm)	
	RMS (nm)	Ra (nm)	RMS (nm)	Ra (nm)
Alq_3	1.694	1.379	1.44	1.144
KI/Alq_3	0.764	0.556	0.757	0.562
Alq_3/C_{60}	1.835	1.341	2.944	1.749
KI/Alq_3/C_{60}	1.77	1.285	2.149	1.404

The XPS analysis was carried out to investigate the effect of KI on the Alq_3 thin layer. Fig.6 shows the survey spectrum of the KI (1nm)/Alq_3 (9nm) sample, from this spectrum we found that no signal can be attributed to iodine (inset of Fig. 6) which shows that there is decomposition of KI during the deposition process.

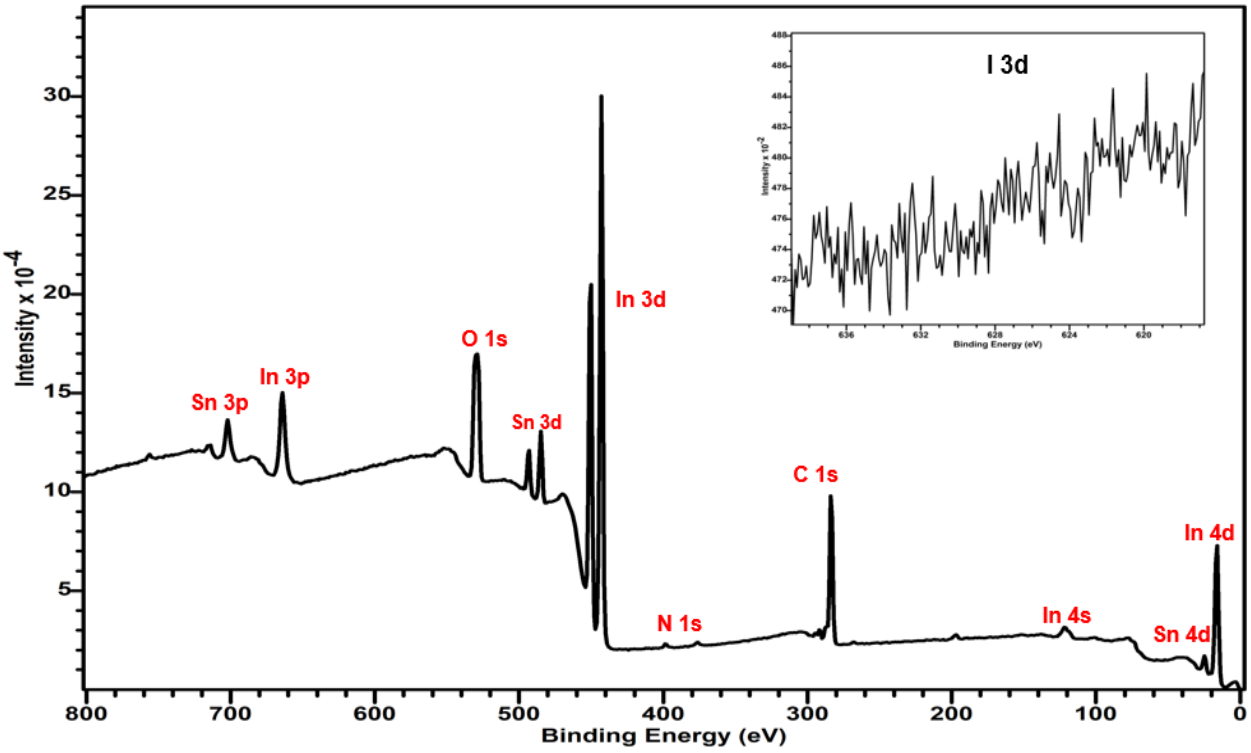

Fig. 6. Survey spectrum of ITO/KI/Alq_3.

Fig.7 displays the carbon core level spectrum where the K_{2p} doublet signal appeared at binding energies 295.4 eV and 292.6eV. Even more interesting, the N1s signal located at a binding energy of 399.3 eV as can be seen in Fig.8. In the presence of K, this signal shifts for higher binding energy by 0.3 eV [39][40]. After Gaussian-Lorentzian fitting an appearance of another peak (A) is observed at low binding energy (397.9 eV) (Fig. 8 (b)), this peak is generated when K is introduced. As already reported by Lee et al, the N1s peak is assigned to N atom in C=N-C bond in pyridyl ring and the peak detected at low binding energy as named here peak (A) is attributed to the strained environment near N atoms in pyridyl ring in Alq_3 that is generated by the K-doped atoms such that the angle changes of C=N-C bond [39]. From this investigation, we can confirm that K diffuses in the Alq_3, which creates a chemical interaction between K and Alq_3 molecules. In the case of the sequence Alq_3/KI, as shown by Fig.8 (c), there is no low binding energy contribution, which explains that there is no improvement of the OPV performance. It was already shown that the Alq_3 isomerization does

not change and retains the same orientation upon the K doping. However, there is a modification of electron distribution [41]. As reported in Ref 30, using K/Alq_3 as cathode buffer layer, the diffusion of K in Alq_3 shifts the valance band of Alq_3 from 1.82 eV to 2.70 eV below the Fermi level. Thus that reduces the electronic injection barrier and consequently improves the Voc value [36]. A similar effect has been shown using Alq_3:K_2CO_3 and Alq_3:Li_2CO_3 as cathode buffer layer in light-emitting diode [40][42]. It was found that the injection barrier was reduced, due to the Alq_3 Fermi level shifts toward the lowest unoccupied molecular orbital (LUMO). This shift results from the increase of anions concentration generated by the chemical reaction between K_2CO_3 and Alq_3 [40]. In our case, the KI is decomposed during sublimation, and only K interacts with Alq_3 molecules**.** Note that the work function of K is equal to 2.5 eV that is lower than the Alq_3 [30], so we can conclude that this interaction between K and Alq_3 as above mentioned may be responsible for the decreasing of the injection barrier between the cathode (ITO) Fermi level and LUMO of the acceptor material (C_{60}) due to decrease in the ITO work function [40][36].

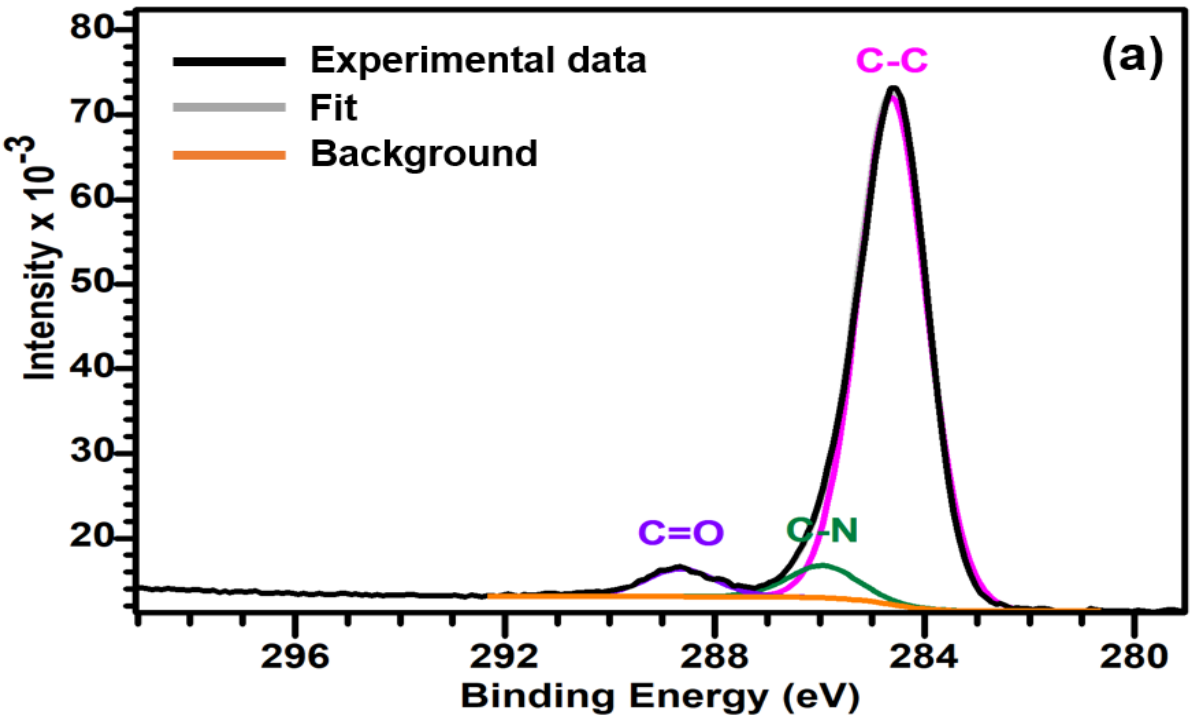

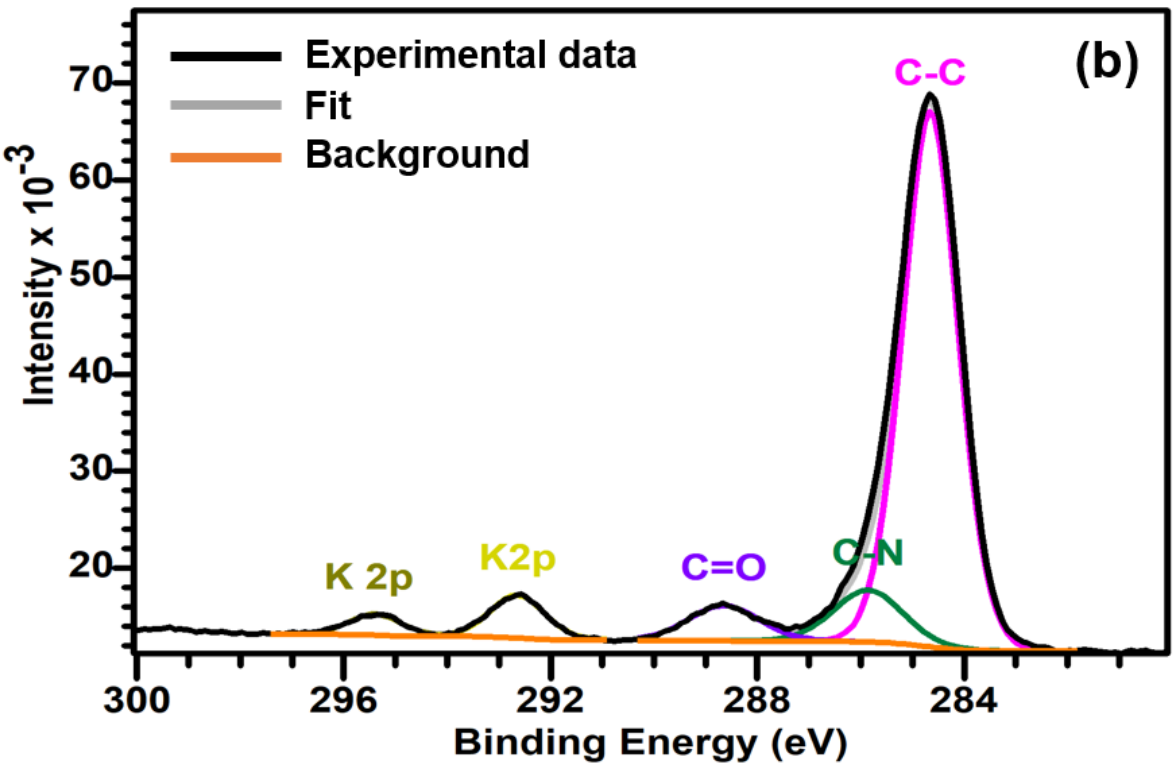

Fig.7.C 1s core level spectrum of (a) Alq3 deposited on bare ITO and (b) Alq3 deposited on ITO/KI.

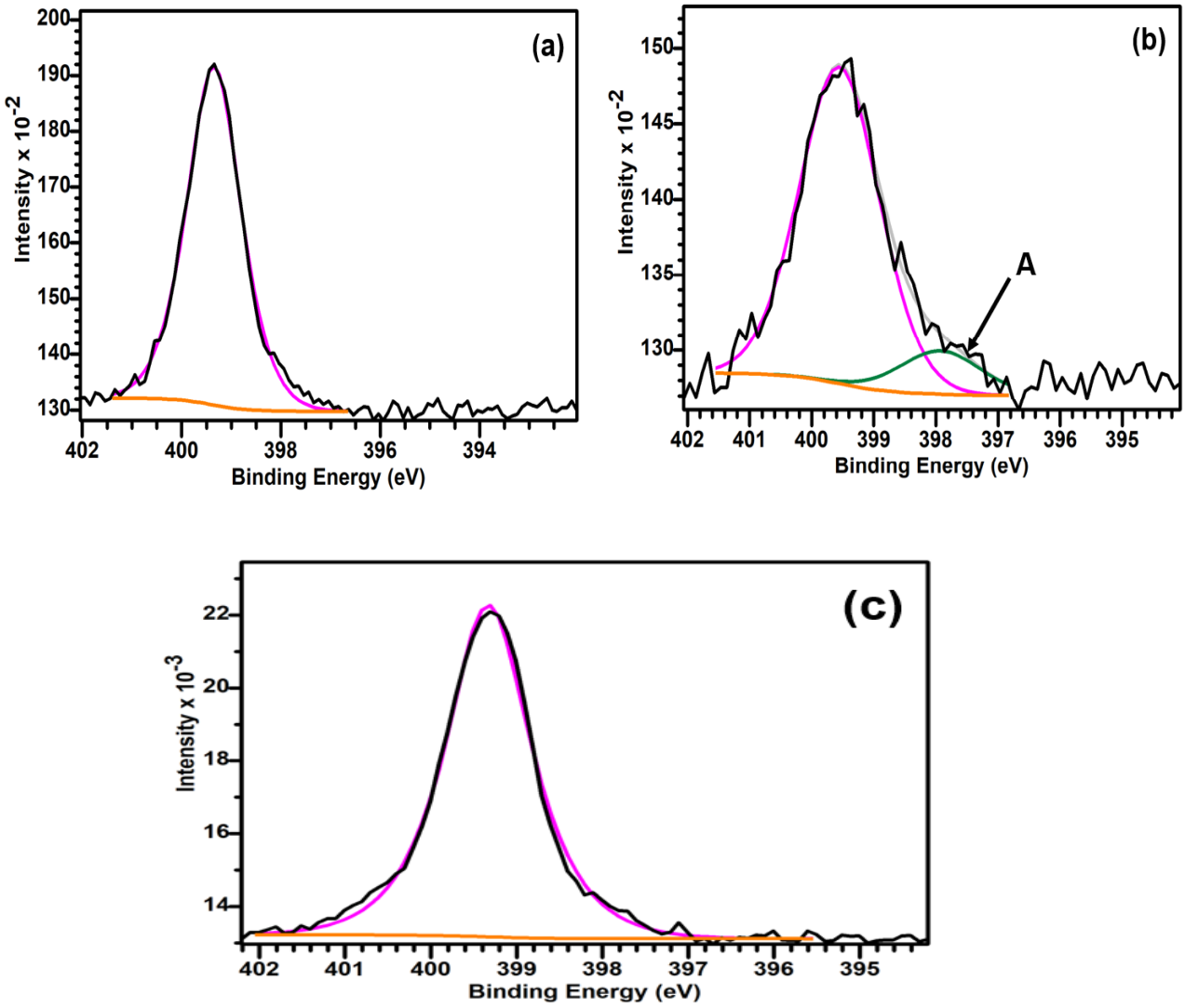

Fig.8. N1s core level spectra of (a) Alq_3 thin layer and (b) KI/Alq_3 thin layer (c) Alq3/KI thin layer.

Moreover, when the thickness of KI is increased to 1.4 nm, the Voc is decreased which induces a reduction of the efficiency to 1.97%, but even so, the fill factor is significantly enhanced compared with device using KI (1nm)/Alq_3 as EBL which indicates that the interfacial recombination's is reduced[22]. For this purpose, we have verified the interfacial properties of C_{60}/CuPc, the structure, and the optical density of the active layers to know the effect of hybrid EBL on the whole device. Fig.9 represents the top-view of SEM images of both samples ITO/EBL/C_{60}/CuPc where EBL is the KI (1nm)/Alq_3 or Alq_3 alone. Without KI thin layer CuPc surface shows a continuous and regular morphology consisted of elongated grains or rods formed on the film surface [43][44]. A transition in the grain's morphology was observed when the KI thin layer is introduced at ITO/Alq_3 interfaces. The grains turn

from rod-like CuPc to spherical grains on the film surface. These spherical grains have a diameter of about 200 nm. The growth of these random grains increases the grain boundaries, which induces defect in the film surface. Thus, they tend to increase the leakage current justifying the slight decrease of the fill factor from 52.5% to 51% for the device without and in the presence of KI, respectively.

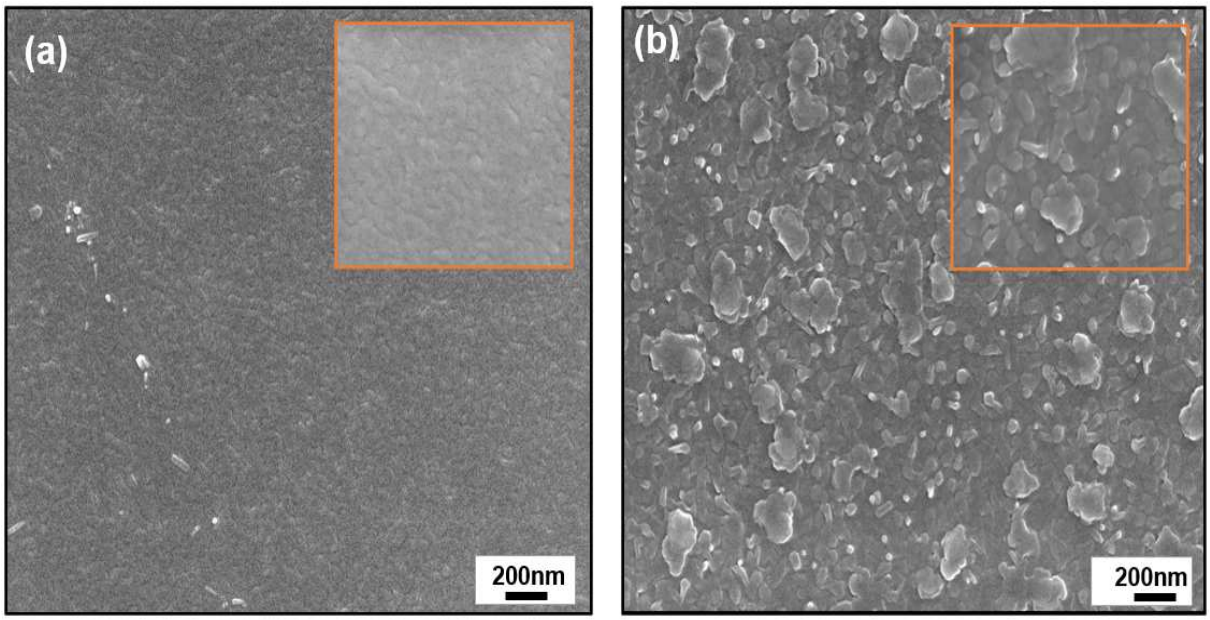

Fig.9. SEM images of (a) ITO/Alq_3/C_{60}/CuPc sample (b) and ITO/KI/Alq_3/C_{60}/CuPc, the inset figures are the magnified images of the same surface film.

Additionally, we have verified the structure of both samples using X-Ray diffraction (Fig.9 (a)). XRD patterns exhibit peaks attributed to ITO thin film. There is no peak diffraction attributed to C_{60} which has an amorphous phase [45], indicating that the C_{60} structure does not change upon the use of KI thin layer. The peak located at $2\theta=6.85°$ is attributed to the crystalline phase α-CuPc corresponding to the diffraction from the (2 0 0) lattice plane indicating that the CuPc molecules stand perpendicular to the substrate [46][44][47][48]. The peak intensity of α-CuPc was significantly increased in the presence of KI thin layer which means that the CuPc crystallinity increases. The UV-visible spectra shown in Fig.9(b) exhibit two absorption peaks at 623 nm and 695 nm in the visible region. They correspond to the Q band (π-π* transition) absorption of CuPc thin film [44]. The absorption of CuPc thin film is slightly increased in the visible region when the KI thin layer is introduced, which is an advantage for increasing the free carrier formation.

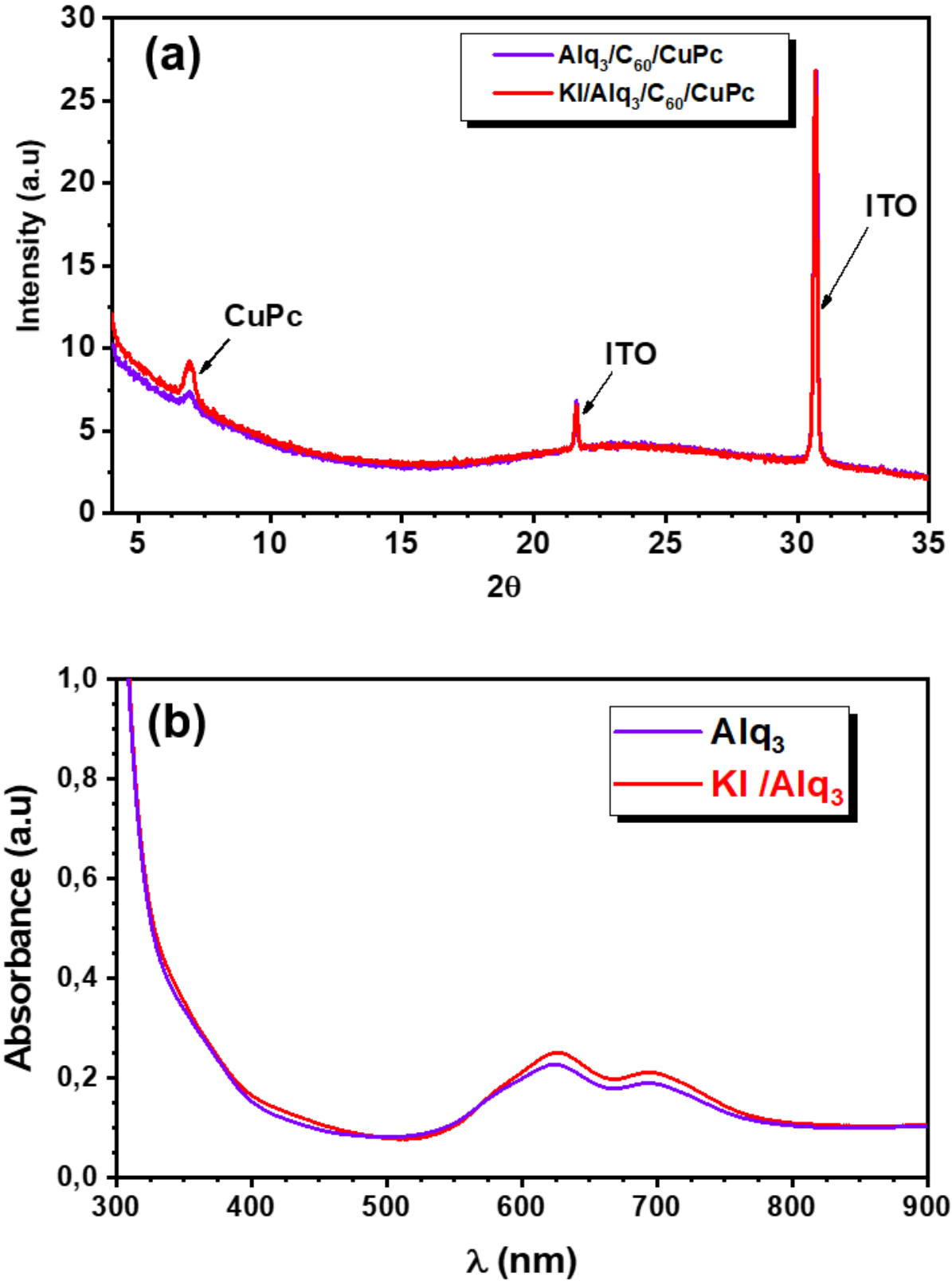

Fig.10. (a) X-ray diffraction and (b) optical absorbance of ITO/ETLs/C_{60}/CuPc where ETL is Alq_3 and KI/Alq_3.

The changes in the structural and optical properties of CuPc thin film with the presence of KI thin layer mainly depend on the under-layer and its microstructure properties. We have checked the C_{60} surface morphology with and without KI thin layer. From the top view of SEM images of C_{60} thin film deposited on ITO/Alq_3 and ITO/KI/Alq_3(Fig.11), we can observe that the whole film surface without KI thin layer is covered with spherical grains, and when KI is introduced, the grains become less dense on the film surface (Fig.11 (b)). For more details about the C_{60} surface morphology, the samples were examined using AFM.

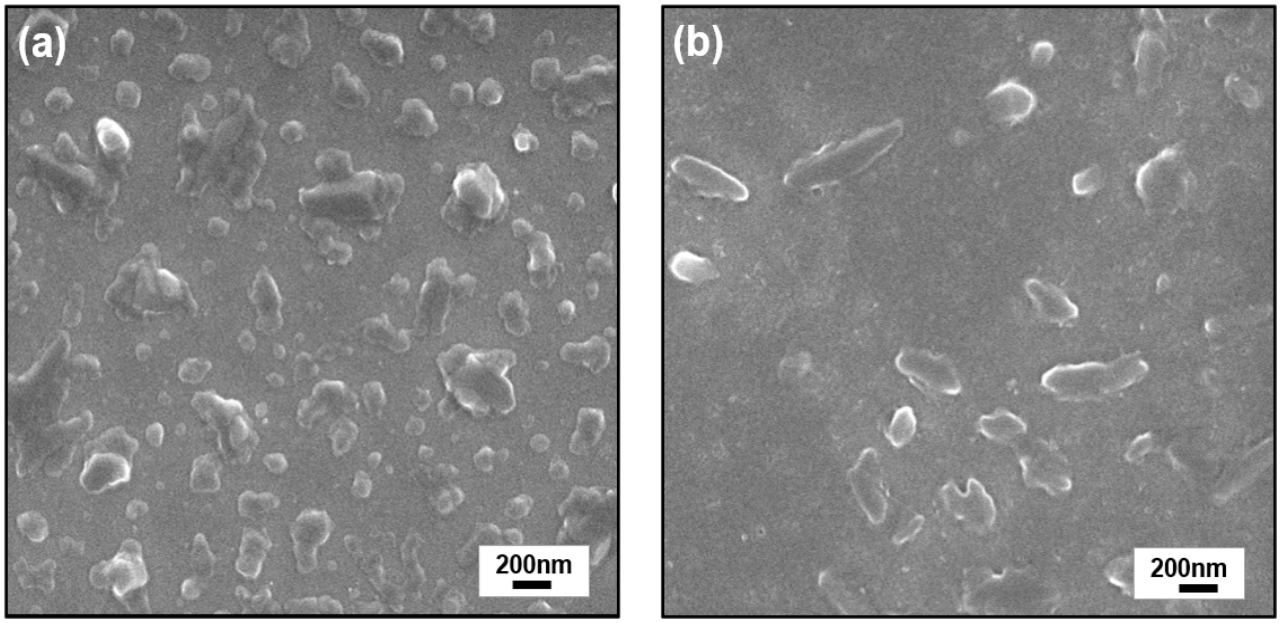

Fig.11. SEM images of (a) ITO/Alq_3/C_{60} and (b) ITO/KI/Alq_3/C_{60}

Fig.12 represent 3D topographies of C_{60} deposited onto ITO/Alq_3 and ITO/KI/Alq_3 and their corresponding profiles. We can see a porous surface with 14 nm as the maximum pit depth for the sample without KI thin layer, while the maximum pit depth value decreased to 11 nm and the porous surface is reduced, which implies a flatter surface in the presence of KI. This flat surface induces a slight decrease in the surface roughness from 2.944 to 2.149 nm. This small decrease of the surface roughness results in a good contact interface between the ED/EA which induces reduction of the leakage current. Such leakage current reduction is advantageous to the Voc enhancement of the OPV [18][49]. On the other hand, the decrease of the roughness may decrease the ED/EA interface area which can cause a decrease of charge separation efficiency.

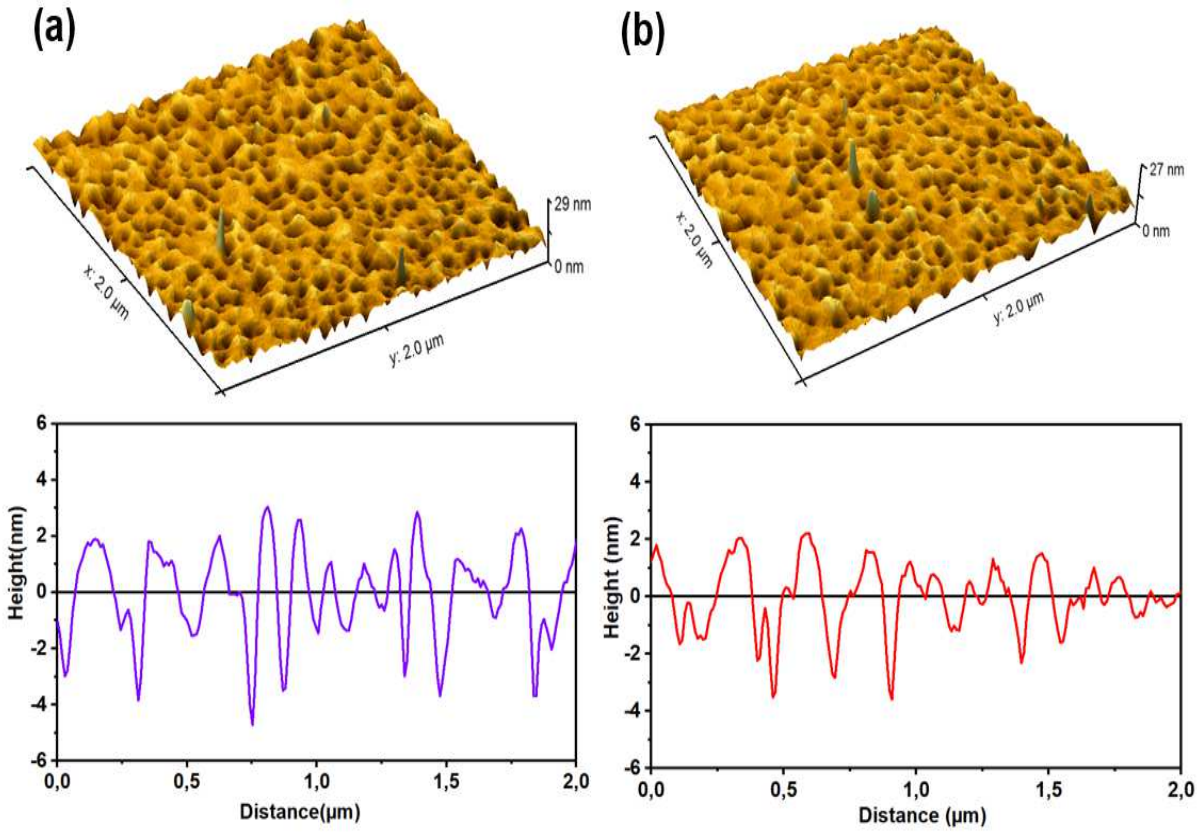

Fig. 12. AFM 3D image (a) ITO/Alq_3/C_{60} (b) ITO/KI/Alq_3/C_{60}.

4. Conclusion

In this study, a hybrid exciton blocking layer or cathode buffer layer and its effect on inverted PHJ-OPVs performances was investigated. This hybrid EBL is composed of potassium iodide (KI) and the well-known Alq_3 thin film. Using XPS analysis, we found that the KI is decomposed during the deposition process and only potassium (K) diffuses in the Alq_3 thin film. The potassium introduced between the ITO and Alq_3 thin film tends to enhance the device efficiency. This reflects that the hybrid EBL KI/Alq_3 can effectively reduce the electron barrier collection at the organic active layer (C_{60}) and the cathode (ITO) interface. We found that the introduction of K enhances the Alq_3 surface smoothness, which has an advantageous effect on the photoactive layer morphology. As shown, upon the insertion of the hybrid EBL, the CuPc crystallinity and its optical properties are enhanced. The effect of KI/Alq_3 on the whole device mostly depends on the thickness of KI inserted. The best performances were obtained by inclusion of 1nm KI thin layer vacuum deposited on the ITO/Alq_3 giving the highest OPV efficiency of 2.2% which is 36% higher than the device with only Alq_3 as EBL. The present works shows that KI/Alq_3 is a very efficient EBL in

OPVs based on the couple CuPc/C_{60}, this work can now be extended to other molecules and other cell configurations to improve OPVs efficiency.

Acknowledgements: We gratefully acknowledge le Partenariat Hubert Curien (PHC) franco-marocain TOUBKAL project, under contract No. 41406ZC for supporting this work.

Reference

[1] Y. Lin, Y. Li, X. Zhan, Small molecule semiconductors for high-efficiency organic photovoltaics, Chem. Soc. Rev. 41 (2012) 4245. https://doi.org/10.1039/c2cs15313k.

[2] Z. Zhang, Y. Lin, Organic Semiconductors for Vacuum-Deposited Planar Heterojunction Solar Cells, ACS Omega. 5 (2020) 24994–24999. https://doi.org/10.1021/acsomega.0c03868.

[3] Y.-A. Su, N. Maebayashi, H. Fujita, Y.-C. Lin, C.-I. Chen, W.-C. Chen, T. Michinobu, C.-C. Chueh, T. Higashihara, Development of Block Copolymers with Poly(3-hexylthiophene) Segments as Compatibilizers in Non-Fullerene Organic Solar Cells, ACS Appl. Mater. Interfaces. 12 (2020) 12083–12092. https://doi.org/10.1021/acsami.9b22531.

[4] Y. Lin, Y. Firdaus, M.I. Nugraha, F. Liu, S. Karuthedath, A. Emwas, W. Zhang, A. Seitkhan, M. Neophytou, H. Faber, E. Yengel, I. McCulloch, L. Tsetseris, F. Laquai, T.D. Anthopoulos, 17.1% Efficient Single-Junction Organic Solar Cells Enabled by n-Type Doping of the Bulk-Heterojunction, Adv. Sci. 7 (2020) 1903419. https://doi.org/10.1002/advs.201903419.

[5] K. Cnops, B.P. Rand, D. Cheyns, B. Verreet, M.A. Empl, P. Heremans, 8.4% efficient fullerene-free organic solar cells exploiting long-range exciton energy transfer, Nat. Commun. 5 (2014) 3406. https://doi.org/10.1038/ncomms4406.

[6] H. Yin, C. Yan, H. Hu, J.K.W. Ho, X. Zhan, G. Li, S.K. So, Recent progress of all-polymer solar cells – From chemical structure and device physics to photovoltaic performance, Mater. Sci. Eng. R Reports. 140 (2020) 100542. https://doi.org/10.1016/j.mser.2019.100542.

[7] K. Nakano, K. Tajima, Organic Planar Heterojunctions: From Models for Interfaces in Bulk Heterojunctions to High-Performance Solar Cells, Adv. Mater. 29 (2017) 1603269. https://doi.org/10.1002/adma.201603269.

[8] F. Gao, A New Acceptor for Highly Efficient Organic Solar Cells, Joule. 3 (2019) 908–909. https://doi.org/10.1016/j.joule.2019.03.027.

[9] G. Zhang, J. Zhao, P.C.Y. Chow, K. Jiang, J. Zhang, Z. Zhu, J. Zhang, F. Huang, H. Yan, Nonfullerene Acceptor Molecules for Bulk Heterojunction Organic Solar Cells, Chem. Rev. 118 (2018) 3447–3507. https://doi.org/10.1021/acs.chemrev.7b00535.

[10] Q. Liu, Y. Jiang, K. Jin, J. Qin, J. Xu, W. Li, J. Xiong, J. Liu, Z. Xiao, K. Sun, S. Yang, X. Zhang, L. Ding, 18% Efficiency organic solar cells, Sci. Bull. 65 (2020) 272–275. https://doi.org/10.1016/j.scib.2020.01.001.

[11] C.J. Schaffer, C.M. Palumbiny, M.A. Niedermeier, C. Jendrzejewski, G. Santoro, S. V. Roth, P. Müller-Buschbaum, A Direct Evidence of Morphological Degradation on a Nanometer Scale in Polymer Solar Cells, Adv. Mater. 25 (2013) 6760–6764. https://doi.org/10.1002/adma.201302854.

[12] K. Wang, X. Song, X. Guo, Y. Wang, X. Lai, F. Meng, M. Du, D. Fan, R. Zhang, G. Li, A.K.K. Kyaw, J. Wang, W. Huang, D. Baran, Efficient as-cast thick film small-molecule organic solar cell with less fluorination on the donor, Mater. Chem. Front. 4 (2020) 206–212. https://doi.org/10.1039/C9QM00605B.

[13] X. He, L. Yin, Y. Li, Design of organic small molecules for photovoltaic application with high open-circuit voltage (V oc), J. Mater. Chem. C. 7 (2019) 2487–2521. https://doi.org/10.1039/C8TC06589F.

[14] Q. Zhang, B. Kan, F. Liu, G. Long, X. Wan, X. Chen, Y. Zuo, W. Ni, H. Zhang, M. Li, Z. Hu, F. Huang, Y. Cao, Z. Liang, M. Zhang, T.P. Russell, Y. Chen, Small-molecule solar cells with efficiency oover 9%, Nat. Photonics. 9 (2015) 35–41. https://doi.org/10.1038/nphoton.2014.269.

[15] R. Po, J. Roncali, Beyond efficiency: Scalability of molecular donor materials for organic photovoltaics, J. Mater. Chem. C. 4 (2016) 3677–3685. https://doi.org/10.1039/c5tc03740a.

[16] https://www.heliatek.com/en/, (2021).

[17] F. Martinez, G. Neculqueo, J.C. Bernède, L. Cattin, M. Makha, Influence of the presence of Ca in the cathode buffer layer on the performance and stability of organic photovoltaic cells using a branched sexithienylenevinylene oligomer as electron donor, Phys. Status Solidi. 212 (2015) 1767–1773. https://doi.org/10.1002/pssa.201431845.

[18] X. Hao, S. Wang, W. Fu, T. Sakurai, S. Masuda, K. Akimoto, Novel cathode buffer layer of Ag-doped bathocuproine for small molecule organic solar cell with inverted structure, Org. Electron. 15 (2014) 1773–1779. https://doi.org/10.1016/j.orgel.2014.04.030.

[19] J.C. Bernède, L. Cattin, M. Morsli, Y. Berredjem, Ultra-thin metal layer passivation of the transparent conductive anode in organic solar cells, Sol. Energy Mater. Sol. Cells. 92 (2008) 1508–1515. https://doi.org/10.1016/j.solmat.2008.06.016.

[20] H. Werner, T. Schedel-Niedrig, M. Wohlers, D. Herein, B. Herzog, R. Schlögl, M. Keil, A.M. Bradshaw, J. Kirschner, Reaction of molecular oxygen with C 60 : spectroscopic studies, J.

Chem. Soc., Faraday Trans. 90 (1994) 403–409. https://doi.org/10.1039/FT9949000403.

[21] Y. Lare, B. Kouskoussa, K. Benchouk, S. Ouro Djobo, L. Cattin, M. Morsli, F.R. Diaz, M. Gacitua, T. Abachi, M.A. del Valle, F. Armijo, G.A. East, J.C. Bernède, Influence of the exciton blocking layer on the stability of layered organic solar cells, J. Phys. Chem. Solids. 72 (2011) 97–103. https://doi.org/10.1016/j.jpcs.2010.11.006.

[22] Z. El Jouad, L. Barkat, N. Stephant, L. Cattin, N. Hamzaoui, A. Khelil, M. Ghamnia, M. Addou, M. Morsli, S. Béchu, C. Cabanetos, M. Richard-Plouet, P. Blanchard, J.C. Bernède, Ca/Alq3 hybrid cathode buffer layer for the optimization of organic solar cells based on a planar heterojunction, J. Phys. Chem. Solids. 98 (2016) 128–135. https://doi.org/10.1016/j.jpcs.2016.06.014.

[23] J. Lee, S. Park, Y. Lee, H. Kim, D. Shin, J. Jeong, K. Jeong, S.W. Cho, H. Lee, Y. Yi, Electron transport mechanism of bathocuproine exciton blocking layer in organic photovoltaics, Phys. Chem. Chem. Phys. 18 (2016) 5444–5452. https://doi.org/10.1039/C5CP07099F.

[24] H. Gommans, B. Verreet, B.P. Rand, R. Muller, J. Poortmans, P. Heremans, J. Genoe, On the Role of Bathocuproine in Organic Photovoltaic Cells, Adv. Funct. Mater. 18 (2008) 3686–3691. https://doi.org/10.1002/adfm.200800815.

[25] W. Na-Na, Y. Jun-Sheng, Z. Yue, J. Ya-Dong, Photocurrent analysis of organic photovoltaic cells based on CuPc/C 60 with Alq 3 as a buffer layer, Chinese Phys. B. 19 (2010) 038602. https://doi.org/10.1088/1674-1056/19/3/038602.

[26] S. Yoo, W.J. Potscavage, B. Domercq, S.-H. Han, T.-D. Li, S.C. Jones, R. Szoszkiewicz, D. Levi, E. Riedo, S.R. Marder, B. Kippelen, Analysis of improved photovoltaic properties of pentacene/C60 organic solar cells: Effects of exciton blocking layer thickness and thermal annealing, Solid. State. Electron. 51 (2007) 1367–1375. https://doi.org/10.1016/j.sse.2007.07.038.

[27] T. Oida, K. Harafuji, Cathode Work Function Dependence of Electron Transport Efficiency through Buffer Layer in Organic Solar Cells, Jpn. J. Appl. Phys. 51 (2012) 091601. https://doi.org/10.1143/JJAP.51.091601.

[28] Z. Liu, M. Tian, N. Wang, Influences of Alq3 as electron extraction layer instead of Ca on the photo-stability of organic solar cells, J. Power Sources. 250 (2014) 105–109. https://doi.org/10.1016/j.jpowsour.2013.10.111.

[29] P. Vivo, J. Jukola, M. Ojala, V. Chukharev, H. Lemmetyinen, Influence of Alq3/Au cathode on stability and efficiency of a layered organic solar cell in air, Sol. Energy Mater. Sol. Cells. 92 (2008) 1416–1420. https://doi.org/10.1016/j.solmat.2008.06.002.

[30] Z. El Jouad, G. Louarn, T. Praveen, P. Predeep, L. Cattin, J.-C. Bernède, M. Addou, M. Morsli, Improved electron collection in fullerene via caesium iodide or carbonate by means of annealing in inverted organic solar cells, EPJ Photovoltaics. 5 (2014) 50401. https://doi.org/10.1051/epjpv/2014003.

[31] J.C. Bernède, L. Cattin, M. Makha, V. Jeux, P. Leriche, J. Roncali, V. Froger, M. Morsli, M. Addou, MoO3/CuI hybrid buffer layer for the optimization of organic solar cells based on a donor–acceptor triphenylamine, Sol. Energy Mater. Sol. Cells. 110 (2013) 107–114. https://doi.org/10.1016/j.solmat.2012.12.003.

[32] T. Kuwabara, C. Iwata, T. Yamaguchi, K. Takahashi, Mechanistic Insights into UV-Induced Electron Transfer from PCBM to Titanium Oxide in Inverted-Type Organic Thin Film Solar Cells Using AC Impedance Spectroscopy, ACS Appl. Mater. Interfaces. 2 (2010) 2254–2260. https://doi.org/10.1021/am100312v.

[33] Y. Lare, M. Banéto, L. Cattin, M. Morsli, K. Jondo, K. Napo, J.C. Bernède, Effect of a zinc oxide, at the cathode interface, on the efficiency of inverted organic photovoltaic cells based on the CuPc/C60 couple, J. Mater. Sci. Mater. Electron. 22 (2011) 365–370. https://doi.org/10.1007/s10854-010-0143-6.

[34] S. Feng, P. Lv, D. Ding, R. A, T. Liu, P. Su, W. Yang, J. Yang, W. Fu, H. Yang, Enhanced photovoltaic property and stability of perovskite solar cells using the interfacial modified layer of anatase TiO2 nanocuboids, Vacuum. 166 (2019) 255–263. https://doi.org/10.1016/j.vacuum.2019.05.025.

[35] H. Schmidt, K. Zilberberg, S. Schmale, H. Flügge, T. Riedl, W. Kowalsky, Transient characteristics of inverted polymer solar cells using titaniumoxide interlayers, Appl. Phys. Lett. 96 (2010) 243305. https://doi.org/10.1063/1.3455108.

[36] L. Cattin, G. Louarn, L. Arzel, N. Stephant, M. Morsli, J.C. Bernède, Power Conversion Efficiency Improvement of Planar Organic Photovoltaic Cells Using an Original Hybrid Electron-Transporting Layer, ACS Omega. 6 (2021) 6614–6622. https://doi.org/10.1021/acsomega.0c05259.

[37] H.-T. Wu, Y. Cheng, C. Leu, S. Wu, C.-F. Shih, Improving Two-Step Prepared CH3NH3PbI3 Perovskite Solar Cells by Co-Doping Potassium Halide and Water in PbI2 Layer, Nanomaterials. 9 (2019) 666. https://doi.org/10.3390/nano9050666.

[38] Z. Li, X. Zhao, X. Lu, Z. Gao, B. Mi, W. Huang, Organic thin-film solar cells: Devices and materials, Sci. China Chem. 55 (2012) 553–578. https://doi.org/10.1007/s11426-011-4400-1.

[39] H.-H. Lee, J. Hwang, T.-W. Pi, Bond cutting in K-doped tris(8-hydroxyquinoline) aluminium,

J. Synchrotron Radiat. 15 (2008) 519–524. https://doi.org/10.1107/S0909049508020013.

[40] P.-C. Kao, C.-C. Chang, S.-Y. Lin, Role of K 2 CO 3 as an n-type dopant in enhancing the electron injection and transport of organic light-emitting devices, Surf. Coatings Technol. 231 (2013) 135–139. https://doi.org/10.1016/j.surfcoat.2012.01.066.

[41] Y. Sakurai, T. Yokoyama, Y. Hosoi, H. Ishii, Y. Ouchi, G. Salvan, A. Kobitski, T.U. Kampen, D.R.T. Zahn, K. Seki, Study of the interaction of tris-(8-hydroxyquinoline) aluminum (Alq3) with potassium using vibrational spectroscopy: Examination of the possible isomerization upon K-doping, Synth. Met. 154 (2005) 161–164. https://doi.org/10.1016/j.synthmet.2005.07.041.

[42] P.-C. Kao, J.-H. Lin, J.-Y. Wang, C.-H. Yang, S.-H. Chen, Improved electron injection into Alq3 based OLEDs using a thin lithium carbonate buffer layer, Synth. Met. 160 (2010) 1749–1753. https://doi.org/10.1016/j.synthmet.2010.06.012.

[43] Y.-S. Hsiao, W.-T. Whang, S.-C. Suen, J.-Y. Shiu, C.-P. Chen, Morphological control of CuPc and its application in organic solar cells, Nanotechnology. 19 (2008) 415603. https://doi.org/10.1088/0957-4484/19/41/415603.

[44] L. Barkat, M. Hssein, Z. El Jouad, L. Cattin, G. Louarn, N. Stephant, A. Khelil, M. Ghamnia, M. Addou, M. Morsli, J.C. Bernède, Efficient hole-transporting layer MoO 3 :CuI deposited by co-evaporation in organic photovoltaic cells, Phys. Status Solidi. 214 (2017) 1600433. https://doi.org/10.1002/pssa.201600433.

[45] M. Rusu, S. Wiesner, T. Mete, H. Blei, N. Meyer, M. Heuken, M.C. Lux-Steiner, K. Fostiropoulos, Organic donor, acceptor and buffer layers of small molecules prepared by OVPD technique for photovoltaics, Renew. Energy. 33 (2008) 254–258. https://doi.org/10.1016/j.renene.2007.05.021.

[46] P. Sullivan, T.S. Jones, A.J. Ferguson, S. Heutz, Structural templating as a route to improved photovoltaic performance in copper phthalocyanine/fullerene (C60) heterojunctions, Appl. Phys. Lett. 91 (2007) 2005–2008. https://doi.org/10.1063/1.2821229.

[47] X.Z. Zhu, C.H. Gao, M.F. Xu, W. Gu, X.B. Shi, Y.L. Lei, Z.K. Wang, L.S. Liao, Enhancement of device efficiency in CuPc/C60 based organic photovoltaic cells by inserting an InCl3 layer, Synth. Met. 162 (2012) 2212–2215. https://doi.org/10.1016/j.synthmet.2012.10.021.

[48] Y. Kinoshita, T. Hasobe, H. Murata, Control of open-circuit voltage in organic photovoltaic cells by inserting an ultrathin metal-phthalocyanine layer, Appl. Phys. Lett. 91 (2007) 083518. https://doi.org/10.1063/1.2775085.

[49] T.J.Z. Stock, T. Ogundimu, J.-M. Baribeau, Z.-H. Lu, J. Nogami, CuPc:C 60 nanocomposite: A pathway to control organic microstructure and phase transformation, Phys. Status Solidi. 252

(2015) 545–552. https://doi.org/10.1002/pssb.201451354.